Munc13-4 reconstitutes calcium-dependent SNARE-mediated membrane fusion

Kristin L. Boswell,[1] Declan J. James,[1] Joseph M. Esquibel,[1] Stephen Bruinsma,[1] Ryutaro Shirakawa,[2] Hisanori Horiuchi,[2] and Thomas F.J. Martin[1]

[1]Department of Biochemistry, University of Wisconsin, Madison, WI 53706
[2]Department of Molecular and Cellular Biology, Institute of Development, Aging and Cancer, Tohoku University, Sendai 980-8575, Japan

Munc13-4 is a widely expressed member of the CAPS/Munc13 protein family proposed to function in priming secretory granules for exocytosis. Munc13-4 contains N- and C-terminal C2 domains (C2A and C2B) predicted to bind Ca^{2+}, but Ca^{2+}-dependent regulation of Munc13-4 activity has not been described. The C2 domains bracket a predicted SNARE-binding domain, but whether Munc13-4 interacts with SNARE proteins is unknown. We report that Munc13-4 bound Ca^{2+} and restored Ca^{2+}-dependent granule exocytosis to permeable cells (platelets, mast, and neuroendocrine cells) dependent on putative Ca^{2+}-binding residues in C2A and C2B. Munc13-4 exhibited Ca^{2+}-stimulated SNARE interactions dependent on C2A and Ca^{2+}-dependent membrane binding dependent on C2B. In an apparent coupling of membrane and SNARE binding, Munc13-4 stimulated SNARE-dependent liposome fusion dependent on putative Ca^{2+}-binding residues in both C2A and C2B domains. Munc13-4 is the first priming factor shown to promote Ca^{2+}-dependent SNARE complex formation and SNARE-mediated liposome fusion. These properties of Munc13-4 suggest its function as a Ca^{2+} sensor at rate-limiting priming steps in granule exocytosis.

Introduction

Ca^{2+}-regulated vesicle exocytosis is essential for signaling in the nervous, endocrine, and immune systems. Mechanisms used in the regulated secretory pathway are conserved across cell types using different members from the Rab, Sec1/Munc18, CAPS (Ca^{2+}-dependent activator protein for secretion)/Munc13, and SNARE protein families that function in the tethering, priming, and fusion of secretory vesicles. Final fusion steps are catalyzed by trans-SNARE complexes assembled between vesicle v-SNARE and plasma membrane t-SNAREs (Jahn and Scheller, 2006). After arrival at the plasma membrane and before fusion, vesicles undergo priming reactions that involve SNARE protein assembly into fusion-competent complexes. In neurons and endocrine cells, members of the CAPS/Munc13 family (Munc13-1 and CAPS-1) mediate vesicle priming reactions (Augustin et al., 1999; Jockusch et al., 2007; Liu et al., 2008). CAPS-1 and Munc13-1 interact with SNARE proteins or with SNARE protein complexes (Guan et al., 2008; Daily et al., 2010). The MHD1 region present in all CAPS/Munc13 proteins

mediates SNARE protein interactions for CAPS-1 (Koch et al., 2000; Khodthong et al., 2011), whereas a larger MHD1/MHD2-containing region was reported to bind SNARE protein complexes in Munc13-1 (Guan et al., 2008).

Munc13-4 is a ubiquitously expressed member of the CAPS/Munc13 family of priming factors whose mechanism is poorly understood. Transcripts for Munc13-4 are present in many cell types (brain, heart, skeletal muscle, kidney, lung, liver, pancreas, and prostate) in which a functional role for Munc13-4 remains to be characterized (Koch et al., 2000). Munc13-4 is highly expressed in cells of the immune system, where it participates in regulated granule exocytosis in cytotoxic T lymphocytes (CTLs), mast cells, neutrophils, and platelets (Feldmann et al., 2003; Shirakawa et al., 2004; Yamamoto et al., 2004; Neeft et al., 2005; Marcenaro et al., 2006; Higashio et al., 2008; Pivot-Pajot et al., 2008). CTLs deficient in Munc13-4 from familial hemophagocytic lymphohistiocytosis (FHL) type 3 (FHL3) individuals fail to exocytose docked cytotoxic granules, which

Correspondence to Thomas F.J. Martin: tfmartin@wisc.edu

Abbreviations used in this paper: ANF, atrial natriuretic factor; CTL, cytotoxic T lymphocyte; FHL, familial hemophagocytic lymphohistiocytosis; MBP, maltose-binding protein; NTA, nitrilotriacetic acid; PC, phosphatidylcholine; PE, phosphatidylethanolamine; PS, phosphatidylserine.

suggested a postdocking role for Munc13-4 in granule priming (Feldmann et al., 2003). Munc13-4 interacts with Rab27a, consistent with a tethering or priming role, although a granule localization has not been established for all cell types expressing Munc13-4 (Shirakawa et al., 2004; Neeft et al., 2005; Elstak et al., 2011). Munc13-4 also localizes to endosomes in CTLs, where it likely functions in the fusion of endosomes for cytotoxic granule maturation (Ménager et al., 2007).

Munc13-4 contains a central MHD1/MHD2 region, but Munc13-4 binding to SNARE proteins has not been reported. The breadth of cell types in which Munc13-4 may function suggests that it might interact broadly with exocytic and possibly endosomal SNARE proteins. Two C2 domains (C2A and C2B) bracket the central domain in Munc13-4, and each is predicted to bind Ca^{2+} ions (Feldmann et al., 2003), but direct Ca^{2+} regulation of Munc13-4 activity has not been demonstrated. Munc13-4 exhibited Ca^{2+}-dependent translocation to the plasma membrane in neutrophils, but it was uncertain whether this was secondary to granule translocation. Munc13-4 binding to liposomes was reported to require C2 domains but was Ca^{2+} independent (Pivot-Pajot et al., 2008). It was important to determine whether Munc13-4 exhibits Ca^{2+}-dependent activity and whether it interacts with exocytic SNARE proteins.

Understanding the mechanisms by which accessory factors regulate SNARE protein function and vesicle exocytosis has been greatly advanced by in vitro studies. Several accessory factors (synaptotagmin-1, Doc2β, Munc18-1, and CAPS-1) bind SNARE proteins and promote lipid mixing in a SNARE-dependent liposome fusion assay (Tucker et al., 2004; Shen et al., 2007; James et al., 2009; Groffen et al., 2010). In the current work, we found that Munc13-4 exhibited C2A-dependent, Ca^{2+}-stimulated SNARE binding and C2B-dependent, Ca^{2+}-stimulated membrane binding. In an apparent coupling of membrane and SNARE binding, Munc13-4 promoted SNARE-dependent liposome fusion in a Ca^{2+}-dependent manner requiring putative Ca^{2+} binding residues in both C2A and C2B domains. Munc13-4 also promoted trans-SNARE complex formation in a Ca^{2+}-dependent manner. These results clarify the mechanism of action of Munc13-4, identify it as a Ca^{2+}-dependent membrane- and SNARE-binding protein, and suggest that Munc13-4 functions as a Ca^{2+} sensor at rate-limiting priming steps in vesicle exocytosis.

Results

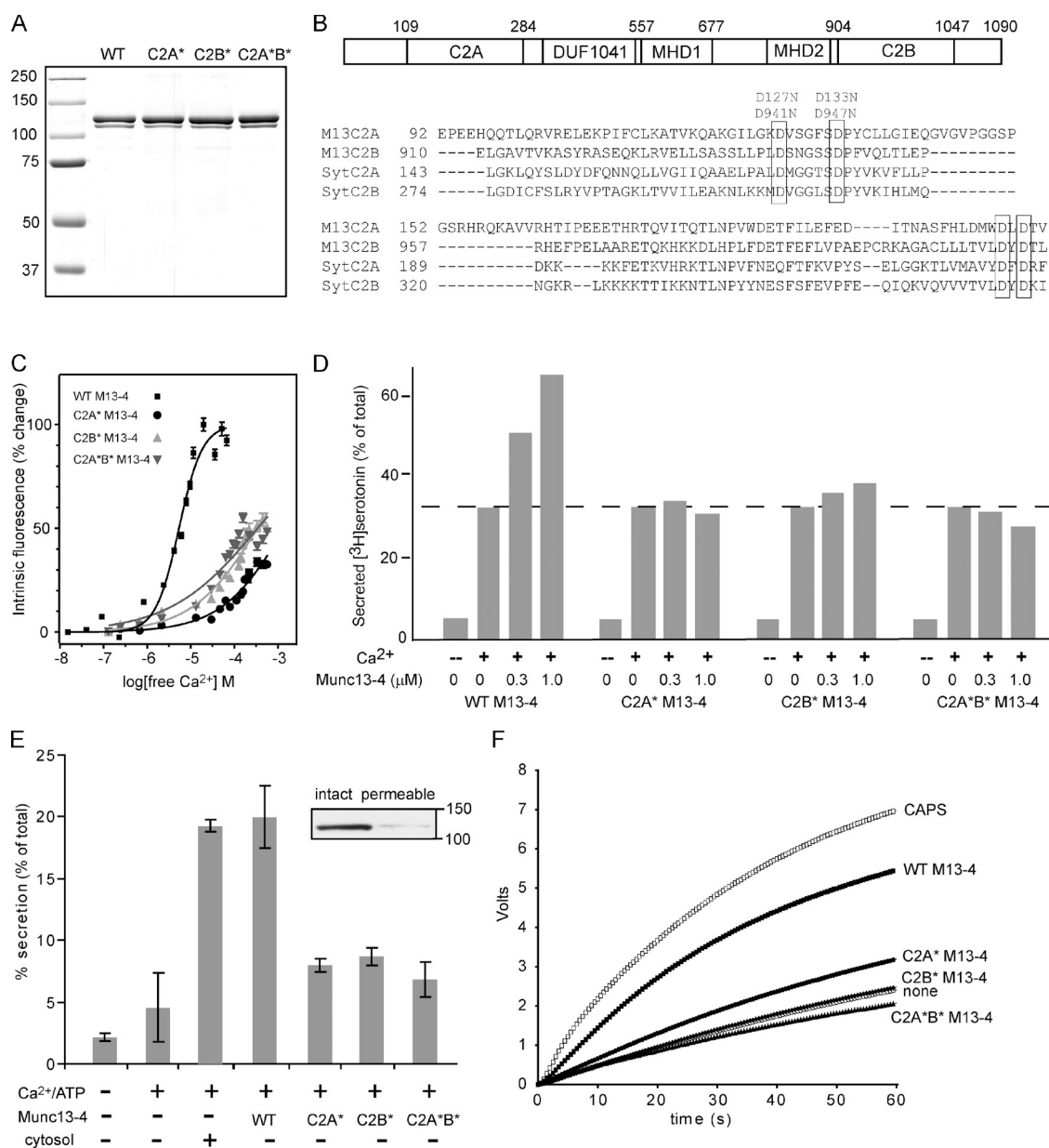### Munc13-4 reconstitutes Ca^{2+}-triggered exocytosis in multiple cell types

Because Munc13-4 is widely expressed, our initial studies examined the activity of Munc13-4 in several cell model systems. We previously showed that Munc13-4 stimulates Ca^{2+}-triggered serotonin secretion in permeabilized platelets (Shirakawa et al., 2004). This and other assays were used to determine whether the activity of Munc13-4 was directly Ca^{2+} regulated. Both C2A and C2B domains of Munc13-4 contain aspartate residues that align with the Ca^{2+}-binding aspartate residues in the C2 domains of synaptotagmin I (Shao et al., 1998), which suggests that Munc13-4 could be a Ca^{2+}-binding protein. To compromise this

potential Ca^{2+} binding, two aspartate residues in the loop 1 region (Fig. 1 B) were mutated to asparagine in either C2A (D127N and D133N) or C2B (D941N and D947N) domains or in both (D127N, D133N, D941N, and D947N). These proteins are termed C2A* Munc13-4, C2B* Munc13-4, or C2A*B* Munc13-4, respectively. Each of the proteins purified as a major band on SDS-PAGE at the expected 120-kD size (Fig. 1 A) and exhibited similar monomer plus dimer mobility on native gels (Fig. S1). Ca^{2+} binding to purified Munc13-4 proteins was measured by monitoring Ca^{2+}-induced changes in the intrinsic fluorescence of aromatic residues (Fig. 1 C). Whereas wild-type Munc13-4 exhibited Ca^{2+}-induced increases in emission with ∼5 µM $[Ca^{2+}]_{1/2}$, the C2A*, C2B*, and C2A*B* Munc13-4 proteins exhibited 10-fold greater $[Ca^{2+}]_{1/2}$ values (Fig. 1 C). These results showed that Munc13-4 is a Ca^{2+}-binding protein and that asparagine for aspartate substitutions in the C2A or C2B domains reduce Ca^{2+} binding–induced increases in the intrinsic fluorescence of Munc13-4.

Permeabilized platelets retained ∼50% of their Munc13-4 (Shirakawa et al., 2004), and the Ca^{2+} stimulation of serotonin release was dependent on the retained Munc13-4 based on the strong inhibition (>75%) by Munc13-4 antibody (Fig. S2). However, the addition of wild-type Munc13-4 further stimulated Ca^{2+}-triggered serotonin secretion from permeable platelets twofold (Fig. 1 D), but C2A* Munc13-4 and C2B* Munc13-4 each failed to do so. Similarly, C2A*B* Munc13-4 was inactive. The results indicate that the stimulation of Ca^{2+}-triggered serotonin secretion by Munc13-4 was dependent on the putative Ca^{2+}-binding residues in the C2A and C2B domains. Thus, Ca^{2+}-dependent dense granule exocytosis in platelets was highly dependent on Munc13-4, which functioned as a Ca^{2+}-binding protein.

These studies were extended to permeable RBL-2H3 mast cells, in which similar results were obtained (Fig. 1 E). RBL-2H3 cells lost >90% of their Munc13-4 upon permeabilization (Fig. 1 E, inset). Ca^{2+}-triggered degranulation was dependent on the addition of cytosol, but purified Munc13-4 substituted for this requirement. In contrast, C2A*B* Munc13-4 was inactive, as were the C2A* and C2B* Munc13-4 proteins (Fig. 1 E). We also assessed Munc13-4 function in permeable neuroendocrine PC12 cells (Fig. 1 F). Washed permeable cells lack Munc13-4 and other soluble priming factors such as CAPS-1. Munc13-4 addition to permeable PC12 cells stimulated Ca^{2+}-triggered catecholamine secretion with an efficacy similar to CAPS-1 (Fig. 1 F). In contrast, neither C2B* or C2A*B* Munc13-4 proteins were functional in the permeable PC12 cell assay, and C2A* Munc13-4 exhibited strongly reduced activity. Thus, in three cell types, Munc13-4 exhibited activity in Ca^{2+}-triggered exocytosis that was dependent on putative Ca^{2+}-binding residues in the C2A and C2B domains. In each assay, 1–10 µM Ca^{2+} was optimal for triggering granule exocytosis, indicating that Munc13-4 exhibits Ca^{2+}-dependent activity over a Ca^{2+} concentration range characteristic of stimulated cells.

These experiments suggested that Munc13-4 may interact with several distinct SNARE proteins. Syntaxin-1, -2, and -4 are the major plasma membrane SNARE proteins required for evoked granule exocytosis in PC12 cells, platelets, and RBL-2H3 mast
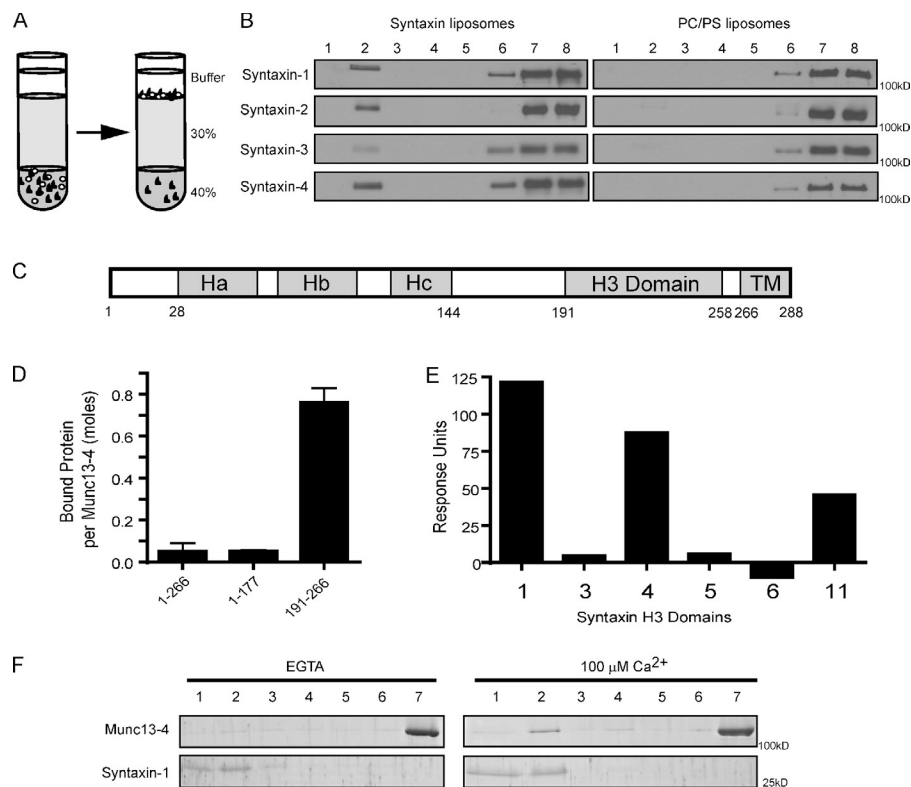
Figure 1. **Munc13-4 reconstitutes Ca²⁺-dependent granule exocytosis in multiple cell types.** (A) Coomassie-stained SDS gels of wild-type (WT) and C2A*, C2B*, and C2A*B* Munc13-4 proteins. A minor degradation fragment was present in some preparations. Molecular mass is indicated in kilodaltons. (B) A schematic representation of the Munc13-4 sequence showing central DUF1041 and MHD1 homology domains present in all CAPS/Munc13 proteins and the MHD2 homology domain conserved in Munc13 proteins. A pileup of sequences from the β1-β2 regions of the C2A and C2B domains of hMunc13-4 and hSynaptotagmin-1 is shown with the conserved aspartate residues in boxes. Positions of the asparagine substitutions in C2A (D127N and D133N) and in C2B (D941N and D947N) are indicated. (C) Ca²⁺ binding to Munc13-4 measured by changes of intrinsic tryptophan fluorescence. 2 μM wild-type, C2A*, C2B*, and C2A*B* Munc13-4 proteins were excited at 280 nm, and emission spectra were collected from 290–390 nm. Normalized plots of the percentage change in fluorescence intensity are shown. These indicated an ∼5 μM $[Ca^{2+}]_{1/2}$ for wild-type Munc13-4, whereas $[Ca^{2+}]_{1/2}$ values for C2A*, C2B*, and C2A*B* Munc13-4 proteins exceeded 300 μM. Mean ± SD values are shown (n = 3). (D) [³H]serotonin release (as a percentage of the total) from preloaded permeable platelets is shown in the absence or presence of 10 μM Ca²⁺ at the indicated concentrations of added wild-type or mutant Munc13-4. The dotted line shows release in the absence of added Munc13-4. Results are representative of three similar experiments. (E) Release of ANF-GFP (as a percentage of the total) from mechanically permeabilized RBL-2H3 cells is shown for incubations without or with 10 μM Ca²⁺, 0.5 mg/ml cytosol, or 10 nM Munc13-4 or C2 domain mutants. Munc13-4 addition without Ca²⁺ was not stimulatory. Results shown are the mean ± SD for triplicate determinations in a single experiment. The inset shows 120-kD Munc13-4 extracted from intact or permeabilized washed RBL-2H3 cells analyzed by SDS-PAGE and immunoblotting. (F) Release of norepinephrine from mechanically permeabilized PC12 cells detected by voltammetry. Incubations at 35°C were conducted in the presence of 20 nM CAPS, 100 nM Munc13-4, or Munc13-4 mutants, as indicated. No release occurs until Ca²⁺ (to ∼1 μM) was injected (at time 0). Each curve represents a single sample. Results are representative of three similar experiments.

cells, respectively (Banerjee et al., 1996; Chen et al., 2000; Paumet et al., 2000). Syntaxin-11 was also proposed as a SNARE protein for exocytosis in CTLs in which Munc13-4 is functional (Bryceson et al., 2007). Because our results implied that Munc13-4 may be capable of functioning on a broad array of SNARE proteins, we directly assessed the SNARE-binding properties of Munc13-4.

Figure 2. **Munc13-4 binds to the H3 region of syntaxins.** (A) Bound and free Munc13-4 were determined by buoyant density flotation of liposomes. (B) 1 µM Munc13-4 was incubated with PC/PS liposomes containing syntaxin-1, -2, -3, or -4 (left) or protein-free PC/PS liposomes (right) for 30 min at room temperature. Bound (fraction 2) and free (fractions 6–8) liposomes were separated on Accudenz gradients and analyzed for Munc13-4 by immunoblotting. Results are representative of two similar experiments. Densitometry with ImageQuant software indicated that bound/free liposomes corresponded to 0.11, 0.06, 0.03, and 0.17 for syntaxin-1, -2, -3, and -4, respectively. (C) Syntaxin-1 contains Habc(28–144), SNARE motif/H3(191–258), and transmembrane(266–288) (TM)domains. (D) Surface plasmon resonance experiments of syntaxin-1 fragments (1–266, 1–177, and 191–266) binding to Munc13-4. Specific binding to Munc13-4 was determined by subtracting background binding to the control MBP. Mean values ± SEM are shown (n = 3). (E) Surface plasmon resonance experiments of the H3 domains of syntaxin-1, -3, -4, -5, -6, and -11. Specific binding to Munc13-4 was determined by subtracting background binding to the control MBP. Results are representative of two similar experiments. (F) 1 µM Munc13-4 was incubated with syntaxin-1–containing liposomes composed of PC/PS/PIP$_2$ (85:12:3) in the presence of EGTA or 100 µM free Ca^{2+}. Accudenz gradient fractions were analyzed by SDS-PAGE and stained with SYPRO ruby.

Munc13-4 binds the H3 domain of multiple syntaxin isoforms

Previous studies used assays with membrane-integrated SNARE proteins to reveal the SNARE-binding properties of CAPS-1 and Munc13-1 (Guan et al., 2008; Daily et al., 2010; Khodthong et al., 2011). Thus, we assessed Munc13-4 binding to membrane-integrated SNARE proteins by buoyant density flotation of liposomes (Fig. 2 A). Phosphatidylcholine (PC)/phosphatidylserine (PS) liposomes reconstituted with different full-length syntaxin proteins were tested. Munc13-4 bound to liposomes containing syntaxin-1, -2, and -4 but only weakly to liposomes containing syntaxin-3 (Fig. 2 B, left). Munc13-4 retention on PC/PS liposomes lacking protein was minimal under these conditions (Fig. 2 B, right).

Syntaxin-1 contains multiple domains (Fig. 2 C), including the N-terminal Habc domain, H3 domain/SNARE motif, and transmembrane domain. To determine which domain interacts with Munc13-4, we used surface plasmon resonance with His$_6$-tagged Munc13-4 (or His$_6$-tagged maltose-binding protein [MBP] as a control) immobilized on a Ni^{2+}–nitrilotriacetic acid (NTA) chip with soluble syntaxin-1 domain proteins as analytes (Fig. 2 D). Munc13-4 retained the H3 domain protein syntaxin-1 (191–266) but not the Habc domain protein syntaxin-1(1–177). Munc13-4 failed to bind the full cytoplasmic domain protein syntaxin-1(1–266), likely because the Habc domain is folded over the H3 domain in this protein (Fig. 2 D). These results were consistent with the finding that the related CAPS-1 and Munc13-1 proteins bind the H3 but not the Habc domain of syntaxin-1 (Daily et al., 2010; Ma et al., 2011; unpublished data).
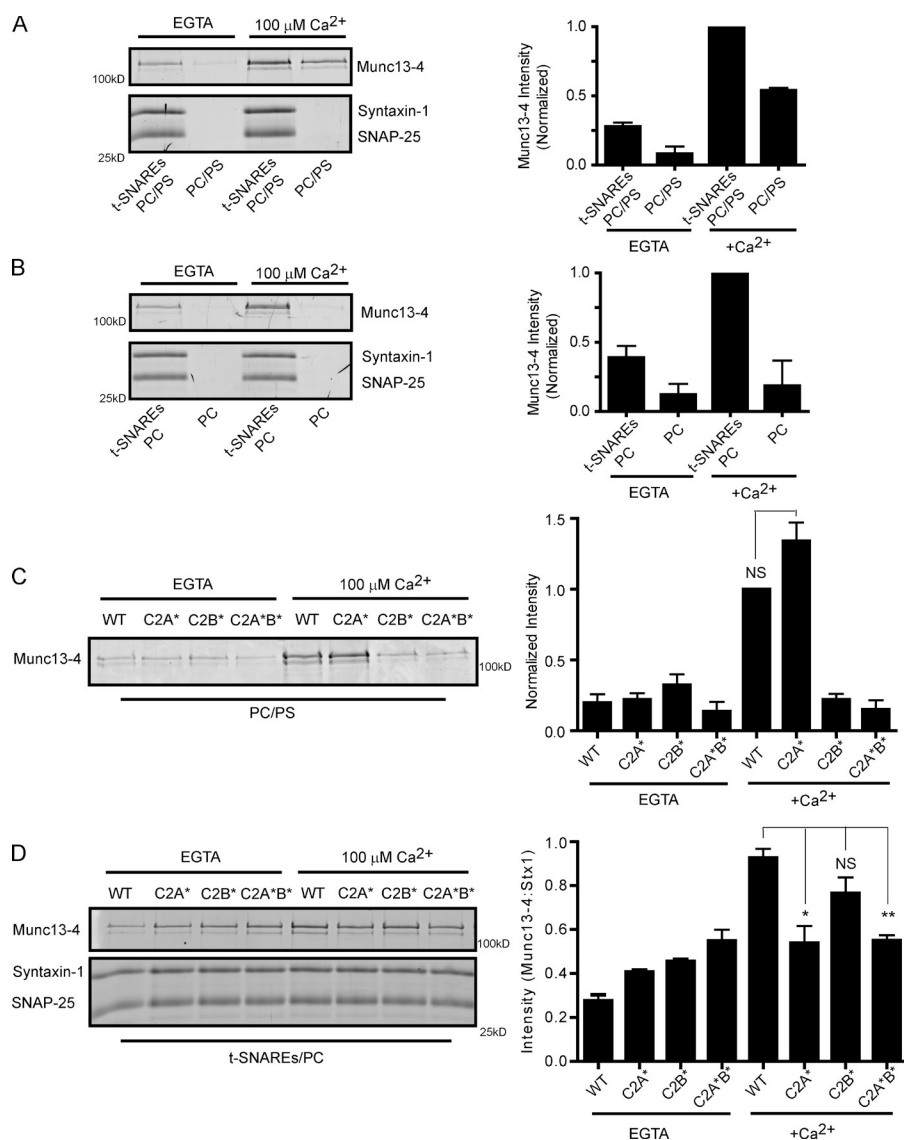
Additional studies showed that Munc13-4 interacts with the H3 domains of syntaxin-1 and -4 but not with the H3 domains of syntaxin-3, -5, or -6 (Fig. 2 E). Collectively, the results indicate that Munc13-4 selectively interacts with exocytic syntaxins (syntaxin-1, -2, and -4) that are present in cell types in which Munc13-4 can regulate exocytosis.

Because syntaxin-11 mutations give rise to an FHL phenotype (FHL4) in CTLs similar to that caused by Munc13-4 mutations (FHL3), it was proposed that Munc13-4 utilizes syntaxin-11 as its effector for cytotoxic granule exocytosis (Bryceson et al., 2007). We found that Munc13-4 does interact with the H3 domain of syntaxin-11 (Fig. 2 E). Pull-down studies confirmed that Munc13-4 binds to GST–syntaxin-11 H3 but not to GST (Fig. S3). Although syntaxin-11 is required for overall cytotoxic T cell activity, this protein localizes to late endosomes and the TGN rather than the plasma membrane (Valdez et al., 1999; Arneson et al., 2007). The Munc13-4 interactions with syntaxin-11 identified here may be involved in endosome fusion (Ménager et al., 2007).

C2 domains differentially mediate Ca^{2+}-dependent SNARE and PS binding

Munc13-4 is a Ca^{2+}-binding protein with two C2 domains that potentially mediate the Ca^{2+} binding (Fig. 1, B and C). The C2 domains of synaptotagmin-1 and related proteins exhibit Ca^{2+}-stimulated binding to acidic phospholipids as well as to t-SNAREs (Pang and Südhof, 2010). We assessed Munc13-4 for similar properties. We initially found that Munc13-4 binding to syntaxin-1–containing liposomes was stimulated by Ca^{2+} (Fig. 2 F).

Figure 3. **Ca²⁺-regulated Munc13-4 binding to t-SNAREs and PS requires C2A and C2B domains, respectively.** (A–D) All binding experiments were conducted by incubating 1 µM Munc13-4 with the indicated liposomes at room temperature for 30 min with EGTA or Ca²⁺ followed by separation of bound and free protein by buoyant density centrifugation conducted in the absence or presence of Ca²⁺. Bound fractions were analyzed by SDS-PAGE, stained with SYPRO ruby, and quantified by densitometry. Munc13-4 migrated between 100- and 150-kD standards. Syntaxin-1 and SNAP-25 migrated between 25- and 37-kD standards. The extent of binding (right graphs) is shown as means ± SEM for $n = 3$. (A) Munc13-4 binding to t-SNARE–containing or protein-free PC/PS liposomes in the presence of EGTA or 100 µM Ca²⁺. (B) Munc13-4 binding to t-SNARE–containing or protein-free PC liposomes in the presence of EGTA or 100 µM Ca²⁺. (C) Binding of wild-type (WT), D127N/D133N, D941N/D947N, and D127N/D133N/D941N/D947N Munc13-4 proteins (termed WT, C2A*, C2B*, and C2A*B* Munc13-4, respectively) to PC/PS liposomes in the presence of EGTA or 100 µM Ca²⁺. Binding of WT and C2A* Munc13-4 to PC/PS liposomes in the presence of Ca²⁺ was not significantly different. (D) Binding of wild-type, C2A*, C2B*, and C2A*B* Munc13-4 proteins to t-SNARE–containing PC liposomes. Munc13-4 binding was normalized to syntaxin-1 (Stx1) content of liposomes. Ca²⁺-stimulated binding of C2A* and C2A*B* Munc13-4 proteins was significantly reduced compared with wild type (*, P < 0.05; **, P < 0.002), whereas binding by C2B* Munc13-4 was not significantly different based on an unpaired t test.
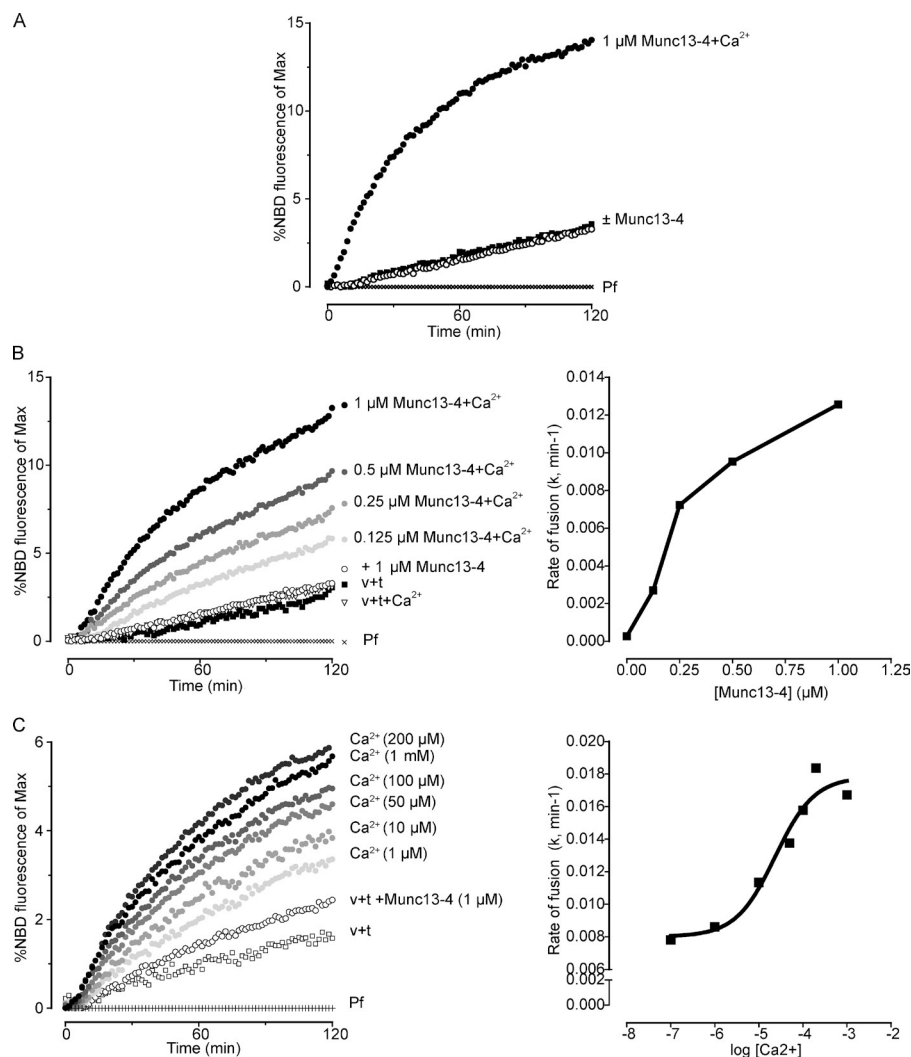
Subsequently, we conducted buoyant density flotation experiments to determine whether Ca²⁺ enhanced the binding of Munc13-4 to t-SNARE–containing liposomes composed of PC/PS. Ca²⁺ was found to stimulate the binding of Munc13-4 to t-SNARE–containing PC/PS liposomes as well as to protein-free PC/PS liposomes (Fig. 3 A). Stimulation by Ca²⁺ was observed at free ionic concentrations as low as 10 µM (unpublished data). The Ca²⁺-dependent binding of Munc13-4 to protein-free liposomes was selective for PC/PS liposomes, whereas binding to PC liposomes was not observed in the absence or presence of Ca²⁺ (Fig. 3 B). However, Munc13-4 exhibited a consistent 2.5-fold increase in binding to t-SNAREs in PC liposomes with Ca²⁺ (Fig. 3 B). The results revealed two Ca²⁺-regulated properties of Munc13-4. Binding to PS-containing membranes was highly dependent on Ca²⁺ (Fig. 3 A), whereas binding to t-SNAREs in PC liposomes occurred in the absence of Ca²⁺ but was stimulated by Ca²⁺ (Fig. 3 B).

It was likely that either one or both of the C2 domains mediated the Ca²⁺ regulation of these Munc13-4 interactions. Therefore, we tested C2 domain mutant proteins for Ca²⁺-dependent

PC/PS liposome binding or for Ca²⁺-stimulated t-SNARE binding in PC liposomes. Mutations in C2A or C2B had little effect on the binding of Munc13-4 to PC/PS liposomes in the absence of Ca²⁺ (Fig. 3 C). In contrast, C2B mutations abrogated the Ca²⁺-dependent interaction of Munc13-4 with PC/PS liposomes, whereas C2A mutations had little effect (Fig. 3 C). As expected, C2A*B* Munc13-4 exhibited no Ca²⁺-dependent binding to PC/PS liposomes. These studies revealed a selective requirement for C2B in the Ca²⁺-dependent interaction of Munc13-4 with acidic phospholipid–containing membranes.

In contrast, experiments in Munc13-4 binding to t-SNARE–containing liposomes in PC revealed a distinctly different basis for Ca²⁺ regulation. The stimulation of t-SNARE binding by Ca²⁺ was similar for wild-type and C2B* Munc13-4 but was largely eliminated for C2A* and C2A*B* Munc13-4 proteins (Fig. 3 D). These experiments revealed a preferential role for C2A in the Ca²⁺-regulated interaction of Munc13-4 with t-SNARE proteins. Overall, these results demonstrated that the Ca²⁺ regulation of membrane binding and SNARE protein binding by Munc13-4 resides with distinct C2 domains.

Figure 4. **Munc13-4 promotes liposome fusion in a calcium-dependent manner.** (A) VAMP-2–containing PC/PS donor liposomes (with NBD-PE and Rh-PE) and t-SNARE–containing PC/PS acceptor liposomes were incubated with 1 µM Munc13-4 in the presence of EGTA or 400 µM free calcium (+Ca^{2+}), as indicated. Control reactions with protein-free (Pf) liposomes replacing t-SNARE liposomes were incubated in parallel for background subtraction. Fusion was detected as increased NBD-PE fluorescence relative to maximal dequenched values. (B) Incubations similar to those of A were conducted at 100 µM Ca^{2+} at the indicated Munc13-4 concentrations (left), and initial fusion rates were determined (right). v + t, reactions with v-SNARE–containing liposomes plus t-SNARE–containing liposomes. (C) Incubations similar to those of A were conducted with 1 µM Munc13-4 at the indicated free Ca^{2+} concentrations (left), and initial fusion rates were determined (right). The EC$_{50}$ for Ca^{2+} was calculated to be 23 ± 4 µM. In all graphs, the curves represent single samples. Results shown are representative of two to four similar experiments.
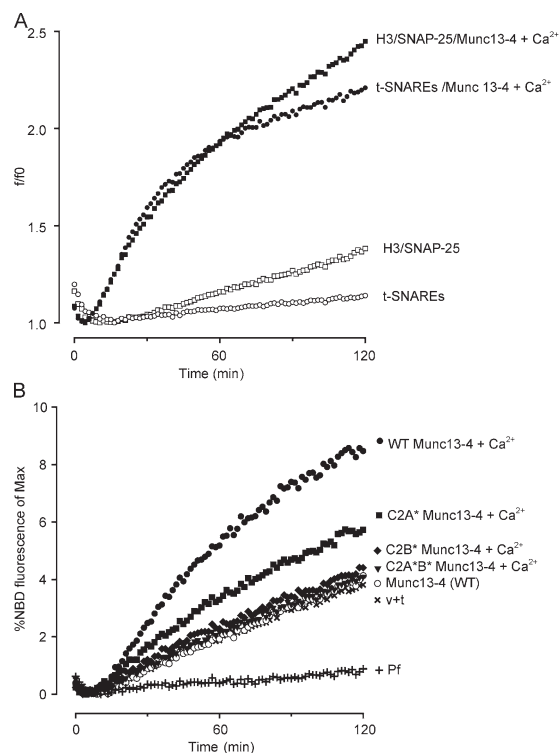
Munc13-4 promotes SNARE-dependent liposome fusion

Previous studies showed that CAPS-1 promotes SNARE-dependent liposome fusion by using membrane interactions mediated by its Pleckstrin homology domain coupled with SNARE protein interactions mediated through its MHD1 domain (James et al., 2009; Khodthong et al., 2011). Munc13-4 contains a C2B domain that mediates membrane interactions as well as an MHD1/MHD2 region that could mediate SNARE binding (Fig. 1 A). Therefore, we determined whether the membrane- and SNARE-binding properties of Munc13-4 would enable it to promote SNARE-dependent liposome fusion. With VAMP-2 donor liposomes and syntaxin-1/SNAP-25 acceptor liposomes, Munc13-4 robustly stimulated the initial rate and final extent of lipid mixing but only in the presence of Ca^{2+} (Fig. 4 A). The Munc13-4 stimulation of lipid mixing was specific for Ca^{2+}, whereas Mg^{2+}, Ba^{2+}, and Sr^{2+} failed to substitute (Fig. S4). Lipid mixing in this assay was previously characterized as full fusion based on contents mixing (James et al., 2009). Rates of fusion exhibited a concentration dependence for Munc13-4 in the presence of Ca^{2+} (Fig. 4 B) and were very similar to those obtained with CAPS-1 in the absence of Ca^{2+}

(not depicted). The Ca^{2+} dependence for Munc13-4 stimulation of liposome fusion exhibited a half-maximal effective concentration (EC$_{50}$) of ~23 µM (Fig. 4 C). The Munc13-4 and Ca^{2+} concentrations needed to promote liposome fusion were higher than those required for function in cells (see Fig. 1), but this minimal fusion assay lacks proteins that may contribute to Munc13-4 localization and activity (e.g., Rab27).

Ca^{2+}-stimulated liposome fusion with Munc13-4 was entirely dependent on SNARE proteins in the donor and acceptor liposomes (Fig. 4, A–C) and was strongly inhibited by the addition of a soluble syntaxin-1 protein (Fig. S5). Because previous binding experiments (Fig. 2 D) showed that Munc13-4 interacted with the H3 rather than the N-terminal Habc domain of syntaxin, we prepared acceptor liposomes reconstituted with an N-terminal–truncated syntaxin-1(191–288) plus SNAP-25 to test with Munc13-4 in liposome fusion. Munc13-4 was found to promote SNARE-dependent liposome fusion with H3/SNAP-25 liposomes in the presence of Ca^{2+} to a similar extent as with full-length syntaxin-1/SNAP-25 liposomes (Fig. 5 A). The results indicated that Munc13-4 interactions with the H3 domain of syntaxin-1 are sufficient for the function of Munc13-4 in SNARE-dependent liposome fusion.

Figure 5. **Munc13-4 utilizes N-terminally truncated syntaxin-1 and requires Ca²⁺-binding C2 domains in SNARE-dependent liposome fusion.** (A) Incubations were conducted in the absence or presence of 1 µM Munc13-4 and 400 µM Ca²⁺, as indicated with DiI-containing VAMP-2 donor liposomes and DiD-containing acceptor liposomes that contained either syntaxin-1 (191–288) with SNAP-25 (H3/SNAP-25) or full-length syntaxin-1(1–288) with SNAP-25 (t-SNARE). Fusion was detected as increased DiD fluorescence expressed relative to the lowest fluorescence as a ratio (f/f₀). Curves show individual samples. Results are representative of three similar experiments. (B) 1 µM wild-type (WT), C2A*, C2B*, or C2A*B* Munc13-4 proteins were incubated with donor v-SNARE liposomes (containing NBD-PE and Rh-PE) and acceptor t-SNARE liposomes, as in Fig. 4 A, with 100 µM Ca²⁺. Fusion was detected as increased NBD-PE fluorescence relative to maximal dequenched values. Curves show individual samples. Results are representative of two similar experiments. v + t, reactions with v-SNARE–containing liposomes plus t-SNARE–containing liposomes.

Both C2 domains are required for Ca²⁺-dependent SNARE-mediated liposome fusion

C2A and C2B domain mutations in Munc13-4 preferentially affected Ca²⁺-dependent SNARE and PS binding, respectively (Fig. 3). We determined whether both of the C2 domains were essential for the Ca²⁺-dependent Munc13-4 stimulation of SNARE-dependent liposome fusion. In the absence of Ca²⁺, all Munc13-4 proteins failed to promote liposome fusion (Fig. 5 B). In the presence of Ca²⁺, wild-type Munc13-4 promoted liposome fusion, whereas C2B* Munc13-4 was completely inactive. This result suggested that Ca²⁺-dependent C2B domain binding to PS is required for Munc13-4 activity in liposome fusion. C2A* Munc13-4 exhibited partial but impaired activity in liposome fusion (Fig. 5 B). This result corresponds to the binding experiments (Fig. 3 D), showing a partial decrease in SNARE binding by C2A* Munc13-4. As expected, the C2A*B* Munc13-4 mutant was completely inactive in Ca²⁺-dependent liposome fusion (Fig. 5 B). Collectively, the results indicate important roles for

the putative Ca²⁺-binding residues in both C2 domains in Munc13-4. They suggest that Ca²⁺-stimulated SNARE binding and Ca²⁺-dependent membrane binding mediated by C2A and C2B domains, respectively, are integrated for the activity of Munc13-4 in SNARE-dependent liposome fusion.
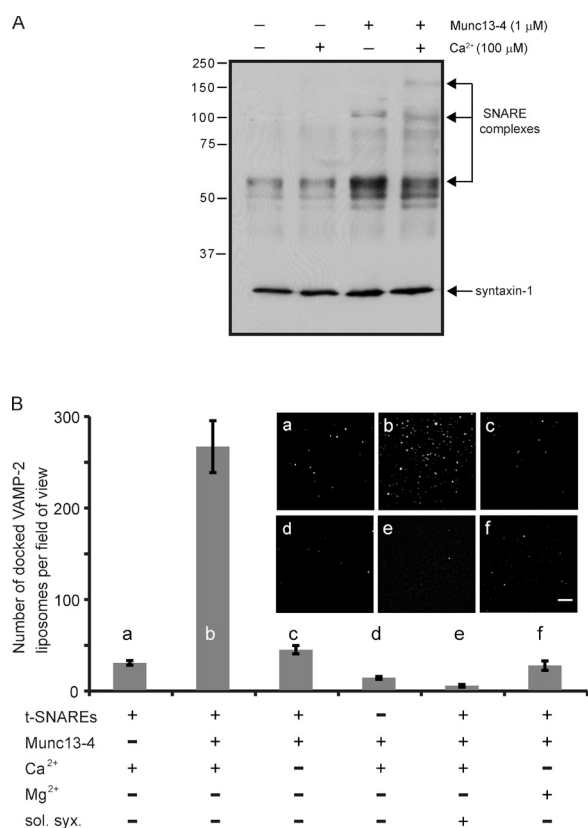
Munc13-4 promotes trans-SNARE complex assembly

CAPS-1 and Munc13-1 function in secretory granule priming steps in neural and endocrine cells (Augustin et al., 1999; Jockusch et al., 2007; Liu et al., 2008). In CTLs, Munc13-4 loss of function was associated with cytotoxic granules that docked at the immunological synapse but did not fuse, suggesting a role in granule priming (Feldmann et al., 2003). The ability of Munc13-4 to promote SNARE-dependent liposome fusion indicates that Munc13-4 can drive trans-SNARE complex assembly. We sought to confirm this prediction in two approaches to detect trans-SNARE complex formation in the absence of fusion. In the first of these, Munc13-4 was incubated with donor v-SNARE and acceptor t-SNARE liposomes on ice to arrest membrane fusion. SNARE protein complexes were detected as SDS-resistant complexes. Munc13-4 was found to promote the formation of ∼70- and ∼110-kD SNARE complexes (Fig. 6 A). In the presence of Ca²⁺, Munc13-4 promoted the formation of ∼165-kD SNARE complexes (Fig. 6 A). The ∼165-kD SNARE protein complex formed by CAPS-1 on liposomes was previously characterized as a dimer of heterotrimeric SNARE complexes (James et al., 2009).

In a second approach, we determined whether v-SNARE (VAMP-2 containing) liposomes would form stable trans-SNARE complexes with t-SNAREs incorporated in a supported bilayer membrane. We found that few v-SNARE liposomes stably dock onto the t-SNARE–containing supported bilayer even when Ca²⁺ is provided (Fig. 6 B, a). In contrast, the addition of Munc13-4 with Ca²⁺ led to a substantial increase in the stable docking of v-SNARE liposomes onto the bilayer (Fig. 6 B, b). The Munc13-4 stimulation of v-SNARE liposome docking was dependent on Ca²⁺ rather than Mg²⁺ and on the presence of SNAREs in both membranes (Fig. 6 B, d and f). Moreover, the addition of an excess of a soluble syntaxin fragment to block trans-SNARE complex formation was found to fully inhibit v-SNARE liposome docking (Fig. 6 B, e). The results indicate that Munc13-4 promotes trans-SNARE complex formation in a Ca²⁺-dependent manner.

Discussion

Munc13-4 plays a role in the regulated exocytosis of secretory granules, especially in cells of hematopoietic origin, but little was known about how it functions. The current work revealed several properties of Munc13-4 that are likely central to its function in regulated secretory pathways. Key properties of Munc13-4 revealed by this work include the Ca²⁺-dependent activity for restoring granule exocytosis to permeable cells that use distinct syntaxins (syntaxin-1, -2, and -4), the ability to directly interact with several exocytic syntaxins (syntaxin-1, -2, and -4), interactions with SNARE proteins regulated by Ca²⁺ and the C2A domain of Munc13-4, binding to acidic phospholipid–containing

Figure 6. **Munc13-4 stimulation of trans-SNARE complex formation is Ca²⁺ dependent.** (A) Munc13-4 stimulates the formation of SDS-resistant SNARE complexes. Incubations with VAMP-2– and syntaxin-1/SNAP-25–containing liposomes were conducted on ice for 30 min with 100 µM Ca²⁺ and 1 µM Munc13-4, as indicated. Reactions terminated in SDS sample buffer without boiling were analyzed by immunoblotting with monoclonal HPC-1 syntaxin-1 antibody. The arrows indicate the positions of ~70-kD, ~120-kD, and ~165-kD SNARE complexes. Similar experiments indicated that VAMP-2 and SNAP-25 comigrated with these complexes. See James et al. (2009) for characterization of SNARE protein complexes. (B) Munc13-4 stimulates the docking of VAMP-2 liposomes onto t-SNARE–containing supported bilayer membranes. VAMP-2 liposomes with Rh-PE were incubated with t-SNARE–containing supported bilayers, and the number of liposomes stably docked for ≥2 min was monitored by total internal reflection fluorescence microscopy. Bar, 5 µm. Incubations contained 1 µM Munc13-4, 200 µM Ca²⁺, or 200 µM Mg²⁺, as indicated. Munc13-4 promoted liposome docking in the presence of Ca²⁺ (b) but not in its absence (c) or with Mg²⁺ (f), nor was liposome docking promoted by Ca²⁺ alone (a). t-SNAREs were required for Munc13-4–promoted docking (d), whereas preincubations of t-SNARE bilayers with 8 µM soluble syntaxin(1–266) (sol. syx.) for 30 min (e) inhibited Munc13-4–promoted docking. Mean values ± SD (n = 3) are shown.

membranes dependent on Ca²⁺ and the C2B domain of Munc13-4, the concerted activity of the C2A and C2B domains of Munc13-4 in promoting Ca²⁺-dependent SNARE-mediated liposome fusion, and the ability to drive trans-SNARE complex formation in a Ca²⁺-dependent manner. These are the properties of a protein that could function as a Ca²⁺ sensor at rate-limiting priming steps in vesicle exocytosis.

Ca²⁺ dependence of Munc13-4 function

Munc13-4 functions in the overall Ca²⁺-dependent process of granule exocytosis. The protein contains two C2 domains predicted to bind Ca²⁺, but there are no previous reports that the activity of Munc13-4 is Ca²⁺ dependent. Earlier studies found that C2

domains are required for Munc13-4 function but not that the C2 domains conferred Ca²⁺-dependent activity. Thus, a Munc13-4 protein lacking both C2 domains localized to recycling endosomes in CTLs but failed to promote endosome merger (Ménager et al., 2007). Similarly, a Munc13-4 protein lacking its C2A domain localized to secretory lysosomes in RBL-2H3 cells but failed to support granule exocytosis (Neeft et al., 2005). C2 domains were also essential for Munc13-4 binding to phospholipids, but this was reported to be Ca²⁺ independent (Pivot-Pajot et al., 2008). The potential importance of C2 domains in Munc13-4 function was also suggested by the identification of missense mutations in Munc13-4 from FHL3 individuals in C2A and C2B domains, but whether these affected Ca²⁺-dependent function was not investigated (Sieni et al., 2011).

The C2A and C2B domains in Munc13-4 both contain canonical Ca²⁺-binding aspartate residues (Fig. 1 A) and exhibit significant homology (~23% identity and 42% similarity) to the second (C2B) C2 domain in Munc13-1. To determine the functional significance of Ca²⁺ binding to Munc13-4, we neutralized two aspartates in the first loop region of each C2 domain to asparagine to generate potential loss of Ca²⁺ binding similar to that for other Ca²⁺-binding C2 domains including Munc13-1 C2B (Shin et al., 2010). We found that all Ca²⁺-dependent properties of Munc13-4 (enhanced intrinsic fluorescence, stimulation of SNARE protein binding, membrane association, and liposome fusion) were eliminated in the C2A*B* Munc13-4 protein. Importantly, the restoration of Ca²⁺-dependent exocytosis by Munc13-4 in permeable platelets, mast cells, and neuroendocrine cells was abolished by mutation of the putative Ca²⁺-binding residues in the C2 domains. The results provide strong evidence that Munc13-4 is a Ca²⁺-dependent protein for its function in granule exocytosis. Moreover, the results indicate that Munc13-4 is a Ca²⁺ sensor for a rate-limiting step in granule exocytosis in the permeable cells.

In double C2 domain proteins in which the C2 domains are tandem, such as in synaptotagmin-1, the Ca²⁺-bound domains interact to affect the overall activity of the protein (Pang and Südhof, 2010). In contrast, the nontandem C2A and C2B domains of Munc13-4 exhibit seemingly independent roles in regulation, but these distinct roles appear to be integrated in the overall Ca²⁺-dependent function of the protein. Thus, putative Ca²⁺ ligand mutations in C2B but not C2A exerted a strong loss of Ca²⁺-dependent phospholipid binding. In contrast, the corresponding mutations in the C2A domain mainly affected Ca²⁺-stimulated SNARE interactions. However, in promoting SNARE-dependent liposome fusion, both C2 domains were required. This indicates that Munc13-4 activity in the liposome fusion assay requires the integration of Ca²⁺-dependent membrane binding (C2B mediated) with Ca²⁺-regulated SNARE binding (C2A mediated). A similar integrated function of both C2 domains is required for Munc13-4 activity in Ca²⁺-dependent granule exocytosis, in which putative Ca²⁺ ligand mutations in either C2 domain largely abrogated activity.

In neural and endocrine cells, a subset of docked secretory vesicles is primed for rapid exocytosis. The Ca²⁺-triggered fusion of primed vesicles is mediated by double C2 domain proteins such as synaptotagmins and Doc2 (Pang and Südhof, 2010). However, other Ca²⁺-dependent regulators such as Munc13-1

function upstream to control vesicle priming reactions (Augustin et al., 1999). Synaptotagmin-2 in mast cells or synaptotagmin-7 in CTLs is proposed to function as a Ca^{2+} sensor for the final step of Ca^{2+}-triggered granule exocytosis (Fowler et al., 2007; Melicoff et al., 2009). However, granules in these cells may not be docked or primed in advance of stimulation and would need to undergo translocation, docking, and priming after cell activation (Pores-Fernando and Zweifach, 2009). The characterization of Munc13-4 as a Ca^{2+}-dependent protein suggests that it functions as an important Ca^{2+} sensor in secretory pathways where secretory granules undergo priming after stimulation.

Role of Munc13-4 in SNARE complex assembly

Extensive molecular genetic studies in hemophagocytic lymphohistiocytic disorders have led to a proposed cascade of events for the docking, priming, and fusion of cytotoxic granules in CTLs (Pachlopnik Schmid et al., 2010). A subset of the proposed protein–protein interactions has been confirmed biochemically. Rab27a (mutated in Griscelli syndrome) is proposed to localize Munc13-4 (mutated in FHL3) in tethering for cytotoxic granule exocytosis (Elstak et al., 2011), and direct Rab27a–Munc13-4 interactions have been reported (Shirakawa et al., 2004; Neeft et al., 2005). Munc18-2 (mutated in FHL5), potentially acting in concert with Munc13-4, is proposed to activate SNARE function by binding to a syntaxin protein. Syntaxin-11 was identified as a loss-of-function allele in FHL4 and has been shown to directly interact with Munc18-2 (zur Stadt et al., 2009) in addition to previously described interactions of Munc18-2 with syntaxin-2 and -3. Our experiments documented for the first time that Munc13-4 directly interacts with syntaxin-11 but also with syntaxin-1, -2, and -4. The role of syntaxin-11 in cytotoxic granule exocytosis by itself is uncertain, and it may function in the fusion of endosomes that participate in the multistep maturation of cytotoxic granules in CTLs after activation (Pachlopnik Schmid et al., 2010). The participation of Munc13-4 in these maturation steps upstream from cytotoxic granule priming (Ménager et al., 2007) suggests that Munc13-4–syntaxin-11 interactions could be important at these earlier steps.

The current work showed that Munc13-4 interacts directly with a broad range of plasma membrane exocytic syntaxins. In our assays, Munc13-4 bound to syntaxin-1, -2, and -4 but exhibited reduced binding to syntaxin-3. We failed to detect binding to the ER syntaxin-5 or to the TGN syntaxin-6. This specificity of binding to exocytic syntaxins was consistent with the ability of Munc13-4 to restore Ca^{2+}-regulated granule exocytosis to a range of permeable cell types that use syntaxin-1, -2, or -4. The interaction of Munc13-4 with syntaxin-1 was mediated through binding to its H3 SNARE domain rather than to the N-terminal Habc domain. CAPS-1 exhibits a similar mode of binding to syntaxin-1 (Daily et al., 2010; Khodthong et al., 2011), and recent work indicates that Munc13-1 also interacts with the syntaxin-1 H3 domain (Ma et al., 2011; unpublished data). A mode of interaction directly with helical SNARE motifs suggests that priming factors in the CAPS/Munc13 family act to stabilize SNARE complexes through direct interactions on the surface of SNARE helical bundles. For Munc13-4 in the current study (Fig. 5) and previously

for CAPS-1 (Daily et al., 2010), interactions with the H3 domain of syntaxin-1 appeared to be sufficient to mediate the stimulation of SNARE-dependent liposome fusion.

For several double C2 domain proteins such as synaptotagmins and Doc2, direct Ca^{2+}-dependent interactions of their C2 domains with SNARE proteins mediate the regulation of membrane fusion (Lynch et al., 2007; Groffen et al., 2010). In contrast, SNARE binding by CAPS-1 and Munc13-1 is mediated by MHD1- and MHD1/MHD2-containing regions of the proteins, respectively (Guan et al., 2008; Khodthong et al., 2011). The possibility that the MHD1/MHD2 region of Munc13-4 mediates SNARE binding remains to be directly assessed. MHD1 is required for Munc13-4 function based on missense mutations that have been characterized in FHL3 patients (Santoro et al., 2006). If the MHD1-containing region mediates SNARE binding in Munc13-4, the regulation of SNARE binding by Ca^{2+} may be through intramolecular C2A–MHD1 interactions. Ca^{2+} binding to C2A may reverse inhibitory interactions with MHD1 that limit SNARE binding. Alternatively, MHD1 might mediate Ca^{2+}-independent SNARE binding, as in CAPS-1, whereas the C2A domain could mediate Ca^{2+}-dependent SNARE binding, as in synaptotagmin or Doc2. Munc13-4 C2A contains a predicted helical region in the putative Ca^{2+}-binding loop 3 similar to that in Munc13-1 C2B (Shin et al., 2010) as well as a unique β3-β4 loop insertion. Potentially, either of these insertions could participate in intramolecular regulation of SNARE binding by MHD1 or direct SNARE binding. Additional studies will be needed to determine the basis for Ca^{2+}-independent and Ca^{2+}-dependent SNARE binding by Munc13-4.

The properties of Munc13-4 revealed by these studies contribute to understanding the general features of the CAPS/Munc13 proteins for promoting vesicle priming and SNARE complex assembly. Separate domains in these proteins mediate membrane binding and SNARE protein binding, which are integrated for overall function to promote SNARE complex formation on membranes. Munc13-4 is the only priming protein in the CAPS/Munc13 family in which membrane binding and SNARE binding are each Ca^{2+} regulated. C2B may mediate direct Ca^{2+}-dependent membrane association, whereas C2A confers Ca^{2+} regulation on SNARE binding. The concerted regulation by C2A and C2B provides a strongly Ca^{2+}-dependent activity for Munc13-4 that would function as a Ca^{2+} sensor in secretory pathways where priming occurs after stimulation.

Materials and methods

Materials
1-palmitoyl, 2-oleoyl PC, 1,2-dioleoyl PS, 1,2-dioleoyl phosphatidylethanolamine (PE), NBD-PE, and N-(lissamine rhodamine B sulfonyl)-1, 2-dipalmitoyl PE (Rh-PE) were purchased from Avanti Polar Lipids, Inc. 1,1′-dioctadecyl-3,3,3′,3′-tetramethylindocarbocyanine perchlorate (DiI) and 1, 1′-dioctadecyl-3,3,3′,3′-tetramethylindodicarbocyanine 4-chlorobenzenesulfonate (DiD) were purchased from Invitrogen. Accudenz was purchased from Accurate Chemical. Rabbit polyclonal antibodies generated against Munc13-4(1–262) or full-length Munc13-4 were produced as previously described (Shirakawa et al., 2004; Murata et al., 2011), and the Munc13-4 (967–980) antibody was obtained from Novus Biologicals.

Plasmids and recombinant proteins
Plasmid constructs pTW34 to express rat syntaxin-1A with N-terminally His-tagged mouse SNAP-25B and pTW2 to express C-terminal His-tagged

mouse VAMP-2 were provided by J.E. Rothman (Yale University, New Haven, CT) and T. Weber (Mount Sinai School of Medicine, New York, NY), and proteins were purified, as previously described (Weber et al., 1998), by Ni-NTA (QIAGEN) chromatography. pGEX-KG to express syntaxin-1(191–267) and constructs to express syntaxin-3, -4, -5, and -6 were provided by R.H. Scheller (Genentech Inc., South San Francisco, CA). cDNA for syntaxin-11 was isolated from cytosolic RNA (RNeasy Midi Kit; QIAGEN) from RBL-2H3 cells and reverse-transcribed using the SuperScript III One-Step reverse transcription kit (Invitrogen). Syntaxin-1, -2, -3, and -4 were cloned into a modified pGEX4T-1 vector (Grishanin et al., 2002). H3 domains for syntaxin-3, -4, -5, and -6 were cloned into pGEX2T with a linker domain between the GST and the H3 domain that mimicked that of pGEX-KG. GST full-length syntaxin-1(1–288), GST–cytosolic syntaxin-1(1–266), GST–SNAP-25, GST–VAMP-2, and GST–syntaxin-1 H3(191–266) were all expressed in *Escherichia coli* and purified on glutathione Sepharose (GE Healthcare). pET28a to express C-terminally His-tagged syntaxin-1A(183–288) was provided by E.R. Chapman (University of Wisconsin, Madison, WI). Expressed syntaxin-1A(183–288) was purified by Ni-NTA (QIAGEN) chromatography. His$_6$-tagged human Munc13-4 protein produced in insect Sf9 cells was purified on Ni-NTA agarose (QIAGEN) and further purified by Mono Q anion exchange chromatography (GE Healthcare), as previously described (Shirakawa et al., 2004).

Preparation of proteoliposomes

Liposomes consisted of 85% PC and 15% PS (termed PC/PS) or 100% PC. For the coflotation assay, dried lipids were hydrated in 25 mM Hepes, pH 7.4, 100 mM KCl, 10% glycerol, and 1 mM DTT (reconstitution buffer) and were forced through a 100-nM pore-sized filter using a Mini-Extruder (Avanti Polar Lipids, Inc.). For syntaxin and t-SNARE liposomes, 100 µl of extruded liposomes was mixed with 200 µl of protein in 25 mM Hepes, pH 7.4, 400 mM KCl, 10% glycerol, 1% β-octylglucoside, and 2 mM β-mercaptoethanol for 30 min, diluted twofold with reconstitution buffer, and then dialyzed overnight against reconstitution buffer containing Bio-Beads (Bio-Rad Laboratories). The liposomes were purified by buoyant density centrifugation on an Accudenz step gradient (3 ml at 40%, 2 ml at 30%, and 0.5 ml at 0% in reconstitution buffer) at 45,000 rpm for 4 h in an SW50.1 rotor (Beckman Coulter). For the lipid-mixing assay, t-SNARE PC/PS liposomes and VAMP-2 liposomes were prepared as previously described (James et al., 2008). In brief, proteoliposomes were formed by comicellization in the presence of either VAMP-2 or coexpressed syntaxin-1A and SNAP-25B, as previously described (Scott et al., 2003). 167 µg SNAP-25/syntaxin-1 in elution buffer (25 mM Hepes-KOH, pH 7.4, 100 mM KCl, 500 mM imidazole-OAc, pH 7.4, and 1.0% β-octylglucoside) was used to resuspend a lipid film containing 1.5 µmol PC/PS in an 85:15 mol ratio to generate liposomes that contained ~40 copies of each SNARE. For fluorescent donor liposomes, ~100 copies of VAMP-2 per liposome were incorporated with a lipid mixture of PC/PS/Rh-PE/NBD-PE at an 82:15:1.5:1.5 mol ratio. Lipid mixtures were spiked with 2 µl [^{3}H]1,2-dipalmitoyl PC (~2 × 10^5 cpm/nmol; DuPont) to determine lipid recoveries and to standardize fusion reactions. In some experiments (e.g., Fig. 5 A), we used alternative fluorescent lipid labeling approaches to report SNARE-dependent vesicle fusion (Smith and Weisshaar, 2011). VAMP-2 liposomes (100 copies/liposome) composed of PC, PS, PE, and DiD at a 76:12:10:2% mol ratio and t-SNARE liposomes with ~40 copies of syntaxin-1A/SNAP-25B or H3(183–288)/SNAP-25B in PC, PS, PIP$_2$, and DiI lipid mixes at a 90:5:3:2% mol ratio were made by comicellization. The DiI/DiD and NBD/Rh assays are interchangeable and gave similar results. All proteoliposomes were dialyzed overnight against reconstitution buffer containing Bio-Beads and purified by Accudenz gradient flotation (Weber et al., 1998; Scott et al., 2003). Proteoliposomes with PC/PS were typically ~50 ± 13 nm, as measured by dynamic light scattering in an N5 submicrometer particle size analyzer (Beckman Coulter). Liposomes were flash frozen in liquid nitrogen and stored at −80°.

Coflotation assay

Liposome coflotation assays were performed as previously described (Weber et al., 1998), with modifications. Liposomes were incubated with Munc13-4 for 30 min at room temperature in 75 µl of reconstitution buffer. Binding reactions to test for Ca^{2+} dependence of Munc13-4 binding to t-SNARES were conducted in the absence of Ca^{2+} (0.2 mM EGTA) or presence of the indicated concentrations of free Ca^{2+}. 75 µl of 80% Accudenz was added to the binding reaction to yield a final concentration of 40% Accudenz. 30% Accudenz and reconstitution buffers were then layered on top and centrifuged for 4 h in an SW50.1 rotor at 45,000 rpm. Either the floated fraction or all fractions were collected and run on SDS-PAGE and analyzed by Western blotting or SYPRO ruby staining. ImageQuant software (GE Healthcare) was used to quantify protein bands.

Lipid-mixing fusion assay

The lipid-mixing assay between fluorescent donor liposomes and nonfluorescent acceptor liposomes was performed as previously described (Weber et al., 1998), with the following modifications. Lipid mixing was reported by the loss of fluorescence resonance energy transfer between fluorescent lipids (NBD-PE and Rh-PE) concentrated in the VAMP-2 liposomes that occurs upon fusion with the nonfluorescent syntaxin-1A/SNAP-25 liposomes. The standard assay used 0.45 mM of acceptor and 0.225 mM of donor liposomes in a total volume of 75 µl of reconstitution buffer without glycerol supplemented with 0.1 mM EGTA. Munc13-4 protein was added at the concentrations indicated in the figure legends. For the stimulation of Munc13-4 acceleration of SNARE-dependent liposome fusion, calcium was added at concentrations, as specified in the figure legends. Blank reactions were prepared for all conditions by substituting syntaxin-1A/SNAP-25 acceptor liposomes with protein-free liposomes to detect non-SNARE–mediated lipid mixing. Reactions were assembled on ice and mixed before addition to 96-well FluoroNunc plates. Lipid mixing was detected by measuring dequenching of NBD fluorescence (excited at 460-nm emission at 538 nm) every 90 s (shaken before each reading) for 2 h at 35°C in a SPECTRAmax GEMINI-XS spectrofluorometer (Molecular Devices). At the end of 2 h, fusion reactions were solubilized with 0.5% wt/vol dodecyl-D-maltoside, and fluorescence readings were recorded for an additional 10 min. Quantification of lipid mixing is expressed as a percentage of a maximal fluorescent signal determined by detergent solubilization normalized by fluorescence of parallel reactions with protein-free liposomes substituting for SNAP-25/syntaxin-1 liposomes to provide a measure of non-SNARE–mediated lipid mixing (James et al., 2008). For vesicle fusion experiments presented in Fig. 5 A, lipid-mixing reactions were assembled using the same buffer and liposome concentrations as in the aforementioned standard assay. Munc13-4 protein and Ca^{2+} were added at the concentrations indicated in the figure legends. Lipid mixing was observed as an increase in fluorescence resonance energy transfer from DiI to DiD labels by measuring DiD (acceptor) fluorescence at 700 ± 5 nm during DiI (donor) excitation at 514 ± 5 nm every 90 s over 2 h at 35°C using the SPECTRAmax GEMINI-XS spectrofluorometer.

Liposome docking assay

Supported bilayers were created on glass slides cleaned by plasma argon scouring for 3 min followed by overnight soaking in NANO-STRIP buffer (Cyantek Inc). Slides were rinsed with an excess of 0.2 µm of filtered Milli-Q water (Millipore) and assembled into Sykes-Moore chambers (BELLCO GLASS). 6 µl of t-SNARE liposomes (1:1 syntaxin1a/SNAP-25 at a lipid/protein ratio of 900, 5% PIP$_2$, and 93.5% PC) labeled with 1.5% dansyl-PE (1,2-dioleoyl-*sn*-glycero-3-phosphoethanolamine-*N*-(5-dimethylamino-1-napthalenesulfonyl) was incubated on the glass for 1 min at 37°C and washed with 5 ml of buffer (25 mM Hepes and 100 mM KCl, pH 7.4). Lipid recovery was confirmed for each bilayer by monitoring fluorescence recovery of dansyl-PE after photobleaching. v-SNARE or protein-free liposomes (85:13.5% mol PC/PS) labeled with 1.5% mol Rh-PE diluted to 0.8 µM lipid in reconstitution buffer were added to t-SNARE–containing planar-supported bilayers with other additions, as indicated, and incubated at room temperature. Bilayers were imaged at room temperature on an inverted microscope (TE2000-U; Nikon) using an Apo total internal reflection fluorescence 100× NA 1.45 objective lens. Images were acquired at 250-ms intervals with an EM charge-coupled device camera (Evolve; Photometrics). Image analysis used MetaMorph software (Universal Imaging).

Surface plasmon resonance

Equimolar amounts of His-tagged MBP and His-tagged Munc13-4 were immobilized on separate flow cells of an Ni-NTA surface plasmon resonance chip (GE Healthcare). The analyte proteins (20 µM) were flowed over the surface of the chip in reconstitution buffer containing 10 mM imidazole using the Biacore 2000 instrument (GE Healthcare). Specific binding to Munc13-4 was determined by subtracting the nonspecific binding to MBP from binding to the Munc13-4 protein at saturation levels. Binding was analyzed using BIAevaluation software (v3.0; GE Healthcare).

Intrinsic protein fluorescence

Protein fluorescence of native aromatic residues was measured in purified full-length wild-type, C2A*, C2B*, and C2A*B* Munc13-4 proteins. Fluorescence measurements with 2 µM Munc13-4 proteins were obtained on an Infinite M1000PRO spectrofluorometer (Tecan Group Ltd.) in 0.02 M Hepes, pH 7.4, 0.1 M NaCl, and 0.00005 M EGTA. Ca^{2+} titrations were performed with a buffered stock solution of CaCl$_2$, and free Ca^{2+} concentrations were determined using WEBMAXC (created by C. Patton, Stanford University, Stanford, CA).

GST pulldown

Binding studies were conducted in 100-µl reactions containing reconstitution buffer, 1% Triton X-100, and 1% cold fish skin gelatin (Sigma-Aldrich). GST and GST–syntaxin-11 H3 domain were bound to glutathione agarose beads overnight at 4°C. 1 µM Munc13-4 was incubated with 1 µM GST or GST–syntaxin-11 H3 domain immobilized on glutathione Sepharose beads. After a 2-h incubation at 4°C, beads were recovered by centrifugation, washed, eluted in sample buffer, and analyzed by SDS-PAGE and Western blotting. GST and GST–syntaxin-11 H3 domain were detected with GST antibody (Sigma-Aldrich), and Munc13-4 was detected with Munc13-4(1–262) antibody and Munc13-4(967–980) antibody (Novus Biologicals).

Permeable cell secretion assays

Platelet degranulation assays were conducted with streptolysin O–permeabilized platelets. Freshly obtained washed platelets were incubated with [^{3}H]serotonin (20,000 cpm/assay; GE Healthcare) to allow uptake into dense-core granules. After washing, platelets were permeabilized with streptolysin O in buffer A (0.05 M Hepes, pH 7.2, 0.078 M KCl, 0.004 M MgCl$_2$, 0.0002 M CaCl$_2$, 0.002 M EGTA, and 0.001 M dithiothreitol) and incubated with an ATP regeneration system and proteins to be tested at 4°C for 30 min followed by 30°C for 2 min. Finally, the platelets were stimulated with 20 µM Ca^{2+} at 30°C for 1 min, and the reaction was stopped by the addition of ice-cold buffer A containing 0.010 M EGTA. Platelets were removed by centrifugation, and [^{3}H]serotonin in the supernatants and pellets was measured by liquid scintillation counting (Shirakawa et al., 2004). Permeable RBL-2H3 and PC12 cell secretion assays were conducted with cells permeabilized by passage through an appropriately fitted ball homogenizer (Grishanin et al., 2004). A stable clone of RBL-2H3 rat mast cells expressing atrial natriuretic factor (ANF) fused to EGFP (ANF-EGFP) was generated by lentiviral transduction. Targeting of ANF-EGFP to secretory granules and cosecretion with the endogenous granule marker β-hexosaminidase were confirmed. Permeable RBL-2H3 and PC12 secretion assays were conducted at 30°C in buffers containing 0.05 M Hepes, 0.12 M K glutamate, 0.002 M EGTA, and 0.1% BSA, pH 7.2, adjusted to 3 µM free Ca^{2+}. Cytosol used in the RBL-2H3 cell assays was prepared from rat brain tissue by homogenization in ice-cold 0.02 M Hepes, pH 7.5, 0.002 M EGTA, 0.001 M EDTA, 0.001 M DTT, 0.0001 M PMSF, and 0.5 µg/ml leupeptin followed by centrifugation at 30,000 g for 30 min and then 100,000 g for 90 min (Walent et al., 1992). After incubation, RBL-2H3 cells were centrifuged at 650 g, and supernatant and 1% Triton X-100–solubilized pellet fractions were assessed for fluorescence in a plate reader (Infinite F500; Tecan Group Ltd.) to determine the percentage of ANF-EGFP secreted. PC12 cell secretion assays detected the release of norepinephrine by rapid disk electrode voltammetry (Grishanin et al., 2004).

Online supplemental material

Fig. S1 shows native gel electrophoresis of purified Munc13-4 proteins. Fig. S2 shows that Munc13-4 antibody inhibits Ca^{2+}-triggered platelet degranulation. Fig. S3 shows pulldown of Munc13-4 binding to GST–syntaxin-11 H3. Fig. S4 shows that Munc13-4 utilizes Ca^{2+} but not Mg^{2+}, Ba^{2+}, or Sr^{2+}. Fig. S5 shows that Munc13-4 stimulation of liposome fusion is dependent on SNARE protein complex formation. Online supplemental material is available at http://www.jcb.org/cgi/content/full/jcb.201109132/DC1.

References

Arneson, L.N., A. Brickshawana, C.M. Segovis, R.A. Schoon, C.J. Dick, and P.J. Leibson. 2007. Cutting edge: Syntaxin 11 regulates lymphocyte-mediated secretion and cytotoxicity. *J. Immunol.* 179:3397–3401.

Augustin, I., C. Rosenmund, T.C. Südhof, and N. Brose. 1999. Munc13-1 is essential for fusion competence of glutamatergic synaptic vesicles. *Nature.* 400:457–461. http://dx.doi.org/10.1038/22768

Banerjee, A., J.A. Kowalchyk, B.R. DasGupta, and T.F. Martin. 1996. SNAP-25 is required for a late postdocking step in Ca2+-dependent exocytosis. *J. Biol. Chem.* 271:20227–20230. http://dx.doi.org/10.1074/jbc.271.45.28294

Bryceson, Y.T., E. Rudd, C. Zheng, J. Edner, D. Ma, S.M. Wood, A.G. Bechensteen, J.J. Boelens, T. Celkan, R.A. Farah, et al. 2007. Defective cytotoxic lymphocyte degranulation in syntaxin-11 deficient familial hemophagocytic lymphohistiocytosis 4 (FHL4) patients. *Blood.* 110:1906–1915. http://dx.doi.org/10.1182/blood-2007-02-074468

Chen, D., A.M. Bernstein, P.P. Lemons, and S.W. Whiteheart. 2000. Molecular mechanisms of platelet exocytosis: Role of SNAP-23 and syntaxin 2 in dense core granule release. *Blood.* 95:921–929.

Daily, N.J., K.L. Boswell, D.J. James, and T.F. Martin. 2010. Novel interactions of CAPS (Ca2+-dependent activator protein for secretion) with the three neuronal SNARE proteins required for vesicle fusion. *J. Biol. Chem.* 285:35320–35329. http://dx.doi.org/10.1074/jbc.M110.145169

Elstak, E.D., M. Neeft, N.T. Nehme, J. Voortman, M. Cheung, M. Goodarzifard, H.C. Gerritsen, P.M. van Bergen En Henegouwen, I. Callebaut, G. de Saint Basile, and P. van der Sluijs. 2011. The munc13-4-rab27 complex is specifically required for tethering secretory lysosomes at the plasma membrane. *Blood.* 118:1570–1578. http://dx.doi.org/10.1182/blood-2011-02-339523

Feldmann, J., I. Callebaut, G. Raposo, S. Certain, D. Bacq, C. Dumont, N. Lambert, M. Ouachée-Chardin, G. Chedeville, H. Tamary, et al. 2003. Munc13-4 is essential for cytolytic granules fusion and is mutated in a form of familial hemophagocytic lymphohistiocytosis (FHL3). *Cell.* 115:461–473. http://dx.doi.org/10.1016/S0092-8674(03)00855-9

Fowler, K.T., N.W. Andrews, and J.W. Huleatt. 2007. Expression and function of synaptotagmin VII in CTLs. *J. Immunol.* 178:1498–1504.

Grishanin, R.N., V.A. Klenchin, K.M. Loyet, J.A. Kowalchyk, K. Ann, and T.F. Martin. 2002. Membrane association domains in Ca2+-dependent activator protein for secretion mediate plasma membrane and dense-core vesicle binding required for Ca2+-dependent exocytosis. *J. Biol. Chem.* 277:22025–22034. http://dx.doi.org/10.1074/jbc.M201614200

Grishanin, R.N., J.A. Kowalchyk, V.A. Klenchin, K. Ann, C.A. Earles, E.R. Chapman, R.R. Gerona, and T.F. Martin. 2004. CAPS acts at a prefusion step in dense-core vesicle exocytosis as a PIP2 binding protein. *Neuron.* 43:551–562. http://dx.doi.org/10.1016/j.neuron.2004.07.028

Groffen, A.J., S. Martens, R. Díez Arazola, L.N. Cornelisse, N. Lozovaya, A.P. de Jong, N.A. Goriounova, R.L. Habets, Y. Takai, J.G. Borst, et al. 2010. Doc2b is a high-affinity Ca2+ sensor for spontaneous neurotransmitter release. *Science.* 327:1614–1618. http://dx.doi.org/10.1126/science.1183765

Guan, R., H. Dai, and J. Rizo. 2008. Binding of the Munc13-1 MUN domain to membrane-anchored SNARE complexes. *Biochemistry.* 47:1474–1481. http://dx.doi.org/10.1021/bi702345m

Higashio, H., N. Nishimura, H. Ishizaki, J. Miyoshi, S. Orita, A. Sakane, and T. Sasaki. 2008. Doc2 alpha and Munc13-4 regulate Ca(2+)-dependent secretory lysosome exocytosis in mast cells. *J. Immunol.* 180:4774–4784.

Jahn, R., and R.H. Scheller. 2006. SNAREs—engines for membrane fusion. *Nat. Rev. Mol. Cell Biol.* 7:631–643. http://dx.doi.org/10.1038/nrm2002

James, D.J., C. Khodthong, J.A. Kowalchyk, and T.F.J. Martin. 2008. Phosphatidylinositol 4,5-bisphosphate regulates SNARE-dependent membrane fusion. *J. Cell Biol.* 182:355–366. http://dx.doi.org/10.1083/jcb.200801056

James, D.J., J. Kowalchyk, N. Daily, M. Petrie, and T.F. Martin. 2009. CAPS drives trans-SNARE complex formation and membrane fusion through syntaxin interactions. *Proc. Natl. Acad. Sci. USA.* 106:17308–17313. http://dx.doi.org/10.1073/pnas.0900755106

Jockusch, W.J., D. Speidel, A. Sigler, J.B. Sørensen, F. Varoqueaux, J.S. Rhee, and N. Brose. 2007. CAPS-1 and CAPS-2 are essential synaptic vesicle priming proteins. *Cell.* 131:796–808. http://dx.doi.org/10.1016/j.cell.2007.11.002

Khodthong, C., G. Kabachinski, D.J. James, and T.F. Martin. 2011. Munc13 homology domain-1 in CAPS/UNC31 mediates SNARE binding required for priming vesicle exocytosis. *Cell Metab.* 14:254–263. http://dx.doi.org/10.1016/j.cmet.2011.07.002

Koch, H., K. Hofmann, and N. Brose. 2000. Definition of Munc13-homology-domains and characterization of a novel ubiquitously expressed Munc13 isoform. *Biochem. J.* 349:247–253. http://dx.doi.org/10.1042/0264-6021:3490247

Liu, Y., C. Schirra, D.R. Stevens, U. Matti, D. Speidel, D. Hof, D. Bruns, N. Brose, and J. Rettig. 2008. CAPS facilitates filling of the rapidly releasable pool of large dense-core vesicles. *J. Neurosci.* 28:5594–5601. http://dx.doi.org/10.1523/JNEUROSCI.5672-07.2008

Lynch, K.L., R.R. Gerona, E.C. Larsen, R.F. Marcia, J.C. Mitchell, and T.F. Martin. 2007. Synaptotagmin C2A loop 2 mediates Ca2+-dependent SNARE interactions essential for Ca2+-triggered vesicle exocytosis. *Mol. Biol. Cell.* 18:4957–4968. http://dx.doi.org/10.1091/mbc.E07-04-0368

Ma, C., W. Li, Y. Xu, and J. Rizo. 2011. Munc13 mediates the transition from the closed syntaxin-Munc18 complex to the SNARE complex. *Nat. Struct. Mol. Biol.* 18:542–549. http://dx.doi.org/10.1038/nsmb.2047

Marcenaro, S., F. Gallo, S. Martini, A. Santoro, G.M. Griffiths, M. Aricó, L. Moretta, and D. Pende. 2006. Analysis of natural killer-cell function in familial hemophagocytic lymphohistiocytosis (FHL): Defective CD107a surface expression heralds Munc13-4 defect and discriminates between genetic subtypes of the disease. *Blood*. 108:2316–2323. http://dx.doi.org/10.1182/blood-2006-04-015693

Melicoff, E., L. Sansores-Garcia, A. Gomez, D.C. Moreira, P. Datta, P. Thakur, Y. Petrova, T. Siddiqi, J.N. Murthy, B.F. Dickey, et al. 2009. Synaptotagmin-2 controls regulated exocytosis but not other secretory responses of mast cells. *J. Biol. Chem.* 284:19445–19451. http://dx.doi.org/10.1074/jbc.M109.002550

Ménager, M.M., G. Ménasché, M. Romao, P. Knapnougel, C.H. Ho, M. Garfa, G. Raposo, J. Feldmann, A. Fischer, and G. de Saint Basile. 2007. Secretory cytotoxic granule maturation and exocytosis require the effector protein hMunc13-4. *Nat. Immunol.* 8:257–267. http://dx.doi.org/10.1038/ni1431

Murata, Y., T. Yasumi, R. Shirakawa, K. Izawa, H. Sakai, J. Abe, N. Tanaka, T. Kawai, K. Oshima, M. Saito, et al. 2011. Rapid diagnosis of FHL3 by flow cytometric detection of intraplatelet Munc13-4 protein. *Blood*. 118:1225–1230. http://dx.doi.org/10.1182/blood-2011-01-329540

Neeft, M., M. Wieffer, A.S. de Jong, G. Negroiu, C.H. Metz, A. van Loon, J. Griffith, N. Krijgsveld, N. Wulffraat, H. Koch, et al. 2005. Munc13-4 is an effector of rab27a and controls secretion of lysosomes in hematopoietic cells. *Mol. Biol. Cell*. 16:731–741. http://dx.doi.org/10.1091/mbc.E04-10-0923

Pachlopnik Schmid, J., M. Côte, M.M. Ménager, A. Burgess, N. Nehme, G. Ménasché, A. Fischer, and G. de Saint Basile. 2010. Inherited defects in lymphocyte cytotoxic activity. *Immunol. Rev.* 235:10–23. (published erratum appears in *Immunol Rev*. 2010. 236:276)

Pang, Z.P., and T.C. Südhof. 2010. Cell biology of Ca2+-triggered exocytosis. *Curr. Opin. Cell Biol.* 22:496–505. http://dx.doi.org/10.1016/j.ceb.2010.05.001

Paumet, F., J. Le Mao, S. Martin, T. Galli, B. David, U. Blank, and M. Roa. 2000. Soluble NSF attachment protein receptors (SNAREs) in RBL-2H3 mast cells: Functional role of syntaxin 4 in exocytosis and identification of a vesicle-associated membrane protein 8-containing secretory compartment. *J. Immunol.* 164:5850–5857.

Pivot-Pajot, C., F. Varoqueaux, G. de Saint Basile, and S.G. Bourgoin. 2008. Munc13-4 regulates granule secretion in human neutrophils. *J. Immunol.* 180:6786–6797.

Pores-Fernando, A.T., and A. Zweifach. 2009. Calcium influx and signaling in cytotoxic T-lymphocyte lytic granule exocytosis. *Immunol. Rev.* 231:160–173. http://dx.doi.org/10.1111/j.1600-065X.2009.00809.x

Santoro, A., S. Cannella, G. Bossi, F. Gallo, A. Trizzino, D. Pende, F. Dieli, G. Bruno, J.C. Stinchcombe, C. Micalizzi, et al. 2006. Novel Munc13-4 mutations in children and young adult patients with haemophagocytic lymphohistiocytosis. *J. Med. Genet.* 43:953–960. http://dx.doi.org/10.1136/jmg.2006.041863

Scott, B.L., J.S. Van Komen, S. Liu, T. Weber, T.J. Melia, and J.A. McNew. 2003. Liposome fusion assay to monitor intracellular membrane fusion machines. *Methods Enzymol.* 372:274–300. http://dx.doi.org/10.1016/S0076-6879(03)72016-3

Shao, X., I. Fernandez, T.C. Südhof, and J. Rizo. 1998. Solution structures of the Ca2+-free and Ca2+-bound C2A domain of synaptotagmin I: Does Ca2+ induce a conformational change? *Biochemistry*. 37:16106–16115. http://dx.doi.org/10.1021/bi981789h

Shen, J., D.C. Tareste, F. Paumet, J.E. Rothman, and T.J. Melia. 2007. Selective activation of cognate SNAREpins by Sec1/Munc18 proteins. *Cell*. 128:183–195. http://dx.doi.org/10.1016/j.cell.2006.12.016

Shin, O.H., J. Lu, J.S. Rhee, D.R. Tomchick, Z.P. Pang, S.M. Wojcik, M. Camacho-Perez, N. Brose, M. Machius, J. Rizo, et al. 2010. Munc13 C2B domain is an activity-dependent Ca2+ regulator of synaptic exocytosis. *Nat. Struct. Mol. Biol.* 17:280–288. http://dx.doi.org/10.1038/nsmb.1758

Shirakawa, R., T. Higashi, A. Tabuchi, A. Yoshioka, H. Nishioka, M. Fukuda, T. Kita, and H. Horiuchi. 2004. Munc13-4 is a GTP-Rab27-binding protein regulating dense core granule secretion in platelets. *J. Biol. Chem.* 279:10730–10737. http://dx.doi.org/10.1074/jbc.M309426200

Sieni, E., V. Cetica, A. Santoro, K. Beutel, E. Mastrodicasa, M. Meeths, B. Ciambotti, F. Brugnolo, U. zur Stadt, D. Pende, et al. 2011. Genotype-phenotype study of familial haemophagocytic lymphohistiocytosis type 3. *J. Med. Genet.* 48:343–352. http://dx.doi.org/10.1136/jmg.2010.085456

Smith, E.A., and J.C. Weisshaar. 2011. Docking, not fusion, as the rate-limiting step in a SNARE-driven vesicle fusion assay. *Biophys. J.* 100:2141–2150. http://dx.doi.org/10.1016/j.bpj.2011.03.015

Tucker, W.C., T. Weber, and E.R. Chapman. 2004. Reconstitution of Ca2+-regulated membrane fusion by synaptotagmin and SNAREs. *Science*. 304:435–438. http://dx.doi.org/10.1126/science.1097196

Valdez, A.C., J.P. Cabaniols, M.J. Brown, and P.A. Roche. 1999. Syntaxin 11 is associated with SNAP-23 on late endosomes and the trans-Golgi network. *J. Cell Sci.* 112:845–854.

Walent, J.H., B.W. Porter, and T.F. Martin. 1992. A novel 145 kd brain cytosolic protein reconstitutes Ca(2+)-regulated secretion in permeable neuroendocrine cells. *Cell*. 70:765–775. http://dx.doi.org/10.1016/0092-8674(92)90310-9

Weber, T., B.V. Zemelman, J.A. McNew, B. Westermann, M. Gmachl, F. Parlati, T.H. Söllner, and J.E. Rothman. 1998. SNAREpins: Minimal machinery for membrane fusion. *Cell*. 92:759–772. http://dx.doi.org/10.1016/S0092-8674(00)81404-X

Yamamoto, K., E. Ishii, M. Sako, S. Ohga, K. Furuno, N. Suzuki, I. Ueda, M. Imayoshi, S. Yamamoto, A. Morimoto, et al. 2004. Identification of novel MUNC13-4 mutations in familial haemophagocytic lymphohistiocytosis and functional analysis of MUNC13-4-deficient cytotoxic T lymphocytes. *J. Med. Genet.* 41:763–767. http://dx.doi.org/10.1136/jmg.2004.021121

zur Stadt, U., J. Rohr, W. Seifert, F. Koch, S. Grieve, J. Pagel, J. Strauss, B. Kasper, G. Nürnberg, C. Becker, et al. 2009. Familial hemophagocytic lymphohistiocytosis type 5 (FHL-5) is caused by mutations in Munc18-2 and impaired binding to syntaxin 11. *Am. J. Hum. Genet.* 85:482–492. http://dx.doi.org/10.1016/j.ajhg.2009.09.005